

NUMERICAL EXPERIMENTS FOR FAMILIES OF L-FUNCTIONS

NICOLÁS COLOMA, FRANCISCO PONCE, GUSTAVO RAMA, AND NATHAN C. RYAN

1. INTRODUCTION

The statistical properties of zeros and central values of L-functions have been extensively studied, computationally, heuristically and analytically. A fruitful approach to studying these statistical properties has been to associate the statistics of an ensemble of matrices from a classical matrix group to the statistics of values of an L-function (or a collection of L-functions). For instance, Montgomery [15] famously conjectured a formula for the pair correlation of the nontrivial zeros of the Riemann zeta function that is the same as formulas for the pair correlation for the eigenvalues of random matrices taken from either the Circular Unitary Ensemble or the Gaussian Unitary Ensemble if one takes the limit as the matrix size goes to infinity. Odlyzko [16] carried out massive computations of zeros of the Riemann zeta function to verify this conjecture. Bogomolny and Keating [2, 3] provided heuristic evidence that not only the pair correlation functions agree, but all the n-point statistics do, as well. Finally, Rudnick and Sarnak [19] proved that the Riemann zeros and the eigenvalues of this random matrix ensemble have the same n-point statistics in a restricted range.

After studying the relationship between the zeros of the zeta function and the eigenvalues of random matrices, analogous work was done with other L-functions and matrix groups. In particular, inspired by the work of Katz and Sarnak [9], collections of L-functions could be placed in families and those families could be associated to matrices from classical matrix groups. Moreover, in these cases it appeared that zeros of the L-functions have the same statistics as the eigenvalues of a randomly chosen matrix from the group, at least up to the leading term. After the work of Katz and Sarnak there quickly appeared many examples of L-functions families behaving in a manner predicted by random matrix theory. Some of the families considered were: L-functions associated to holomorphic cusp forms (in either weight or level aspect); Dirichlet L-functions (either all or quadratic); and various twists or symmetric powers of L-functions. Analytic results about low-lying zeros were shown by Iwaniec, Luo, and Sarnak [8], Rubinstein, Özlük and Snyder [17], and others.

In this paper we focus on families of quadratic twists of L-functions of holomorphic modular forms. In particular, we want to understand the distribution of their low-lying zeros. Miller [14, Figs. 3 & 4] observed that the first normalized zero above the central point of L-functions attached to rank-0 elliptic curves was repulsed from the central point. Dueñez, Huynh, Keating, Miller, and Snaith record [7, Fig. 4] a similar repulsion in the family of even quadratic twists of the elliptic curve E_{11} . Also in [7], they consider an “excised” model in which, because of a zero free region near $s = 1/2$ guaranteed by theorems of Waldspurger [23] and Kohnen–Zagier [11], they only consider eigenvalues above a certain cutoff. They give explicit formulas for the size of the matrices to be used in both the “standard” and the excised models and the cutoff for the excised model. In a recent preprint of Barrett and Miller [1], similar analytic work is done for families of quadratic twists that do not correspond to the unitary group as families of twists of elliptic curves do. In this paper, we numerically verify the conjectured formulas for these families.

The paper is organized as follows. In the next section, we give the necessary random matrix theory and L-function background and we summarize the main results in [1]. In the subsequent section we describe the computations we carried out and the describe our results.

2. NUMERICAL EXPERIMENTS

In this section we perform preliminary experiments investigating whether there is similar repulsion if E_{11} is replaced with either (i) a cusp form f of weight > 2 with trivial nebentypus, (ii) a cusp forms f with complex multiplication by its own nontrivial nebentypus ($f = \bar{f}$) or (iii) a cusp form f with nontrivial nebentypus ($f \neq \bar{f}$). The L-function calculations were carried out in PARI/GP [22] and the random matrix theory calculations were carried out in Sage [21]; the plots and statistics were done in R [18]. The random matrix theory calculations were based on the algorithms in [13]. Our code is available at [20]. We use LMFDB labels [12] to identify our forms.

2.1. Density Plots of Zeroes.

2.1.1. *Trivial nebentypus.* Fix f to be a cusp form of level 3 and weight 8 (LMFDB label: **3.8.a.a**). Let d be an admissible discriminant as in [[NCR: Definition 4]] for χ_f principal; further assume that $L(1/2, f \otimes \psi_d) \neq 0$. We calculate the distribution of the lowest zero for $L(s, f \otimes \psi_d)$ for all $d < X$ for $X = 40000$. The basic statistics of the distributions are reported in Table 1 and density plots for the distributions are seen in Figure 1. As expected, the center of the distribution shifts to the left as d increases.

	$d < 24231$	$24231 \leq d < 40000$
Min	0.0007601	0.0000216
1Q	0.0484906	0.0420084
Median	0.1042420	0.0874339
Mean	0.1186840	0.1021103
3Q	0.1707843	0.1468551
Max	0.5887751	0.3981730

TABLE 1. The minimum, 1st quartile, median, mean, 3rd quartile and maximum of the imaginary parts of the first zero of $L(f \otimes \psi_d, s)$ above the central value for $f \in M_8(\Gamma_0(3))$ of trivial nebentypus and for quadratic characters ψ_d of admissible discriminant d . We have a cut off at $d = 24231$ because that d corresponds to a change in the size of the corresponding matrices as well, from $N = 8$ to $N = 9$.

2.1.2. *Self-dual, non-trivial nebentypus.* Let $q = e^{2\pi iz}$, and let

$$f(z) = q \prod_{n=1}^{\infty} (1 - q^n)^3 (1 - q^{7n})^3.$$

Then f is a cusp form and a newform of weight 3, level 7 with character $\chi = \left(\frac{n}{7}\right)$, and has Fourier coefficients that are all real (LMFDB label: **7.3.b.a**). The construction of f follows from a general construction of Shimura, and f arises from a Hecke größencharakter. Let $\mathcal{D}(X)$ be as in Definition 4, self-CM case, with the choice $\heartsuit = \pm 1$. We calculate the distribution of the lowest zero for $L(s, f \otimes \psi_d)$ for $d < X$ for $X = 40000$ and for each value of \heartsuit . The basic statistics of the distributions are reported in Table 2 and density plots for the distributions are seen in Figure 2. As expected, the center of the distribution decreases as d increases.

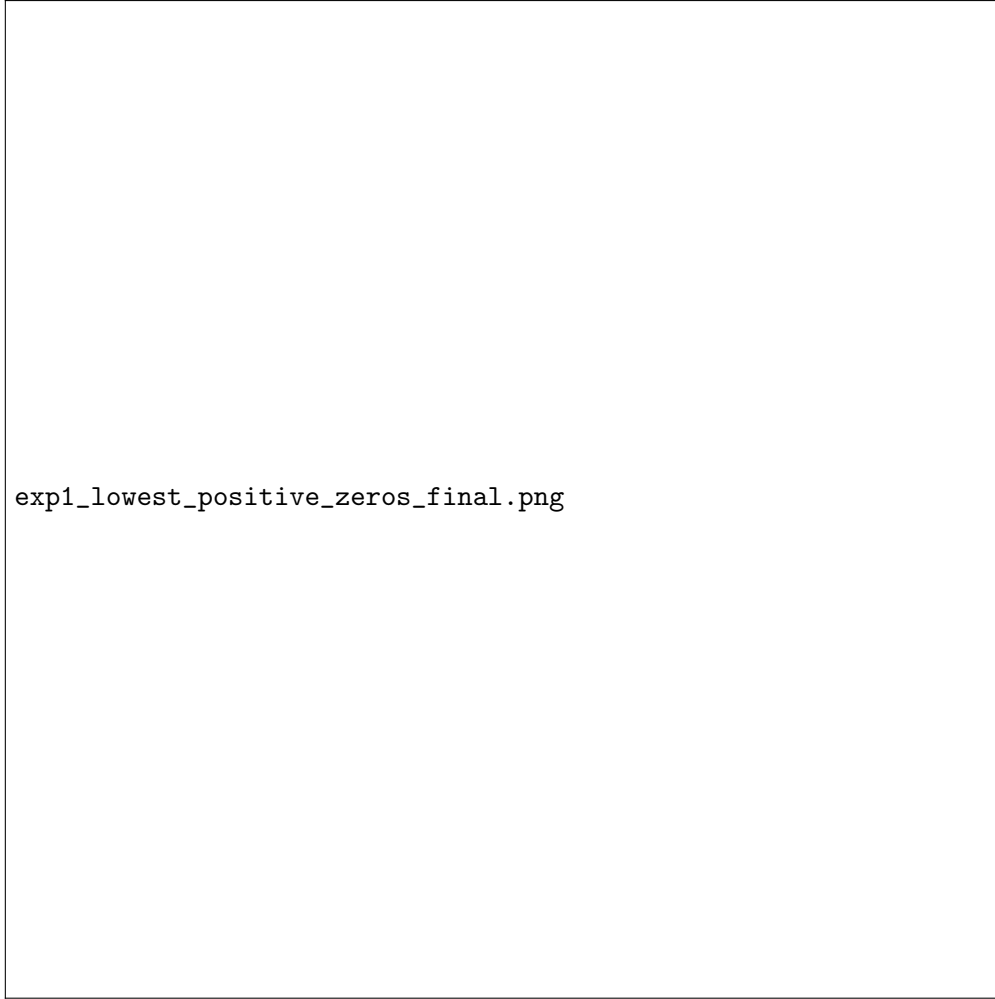
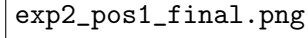


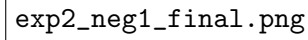
FIGURE 1. Density plots of imaginary parts of the first zero of $L(f \otimes \psi_d, s)$ above the central value for $f \in M_8(\Gamma_0(3))$ of trivial nebentypus and for quadratic characters ψ_d of admissible discriminant d . The dashed line corresponds to the mean of the sample. The panel on the bottom corresponds to $d < 24231$ and the panel on the top corresponds to $24231 \leq d < 40000$.

	$d < 24231$ $\heartsuit = +1$	$24231 \leq d < 400000$ $\heartsuit = +1$	$d < 24231$ $\heartsuit = -1$	$2431 \leq d < 400000$ $\heartsuit = -1$
Min	0.010538	0.019815	0.019895	0.020768
1Q	0.168014	0.149512	0.200736	0.177042
Median	0.228307	0.202696	0.268618	0.237885
Mean	0.234366	0.204902	0.275567	0.238701
3Q	0.296316	0.259163	0.344169	0.296742
Max	0.781105	0.480717	1.297081	0.502771

TABLE 2. The minimum, 1st quartile, median, mean, 3rd quartile and maximum of the imaginary parts of the first zero of $L(f \otimes \psi_d, s)$ above the central value for of trivial nebentypus and for quadratic characters ψ_d of admissible discriminant d .



exp2_pos1_final.png



exp2_neg1_final.png

FIGURE 2. Density plots of imaginary parts of the first zero of $L(f \otimes \psi_d, s)$ above the central value for $f \in M_3(\Gamma_0(7))$ of trivial nebentypus, for quadratic characters ψ_d of admissible discriminant d . The top image is for $\heartsuit = +1$ and the bottom image is for $\heartsuit = -1$. The dashed line corresponds to the mean of the samples.

	$1 < d < 22897$ $\diamond = 1$	$22897 \leq d < 40000$ $\diamond = 1$	$1 < d < 22897$ $\diamond = 7$	$22897 \leq d < 40000$ $\diamond = 7$
Min	0.005661	0.001134	0.004753	0.00136
1Q	0.119455	0.095061	0.092193	0.08686
Median	0.192202	0.163135	0.171398	0.16207
Mean	0.217638	0.180711	0.219049	0.19592
3Q	0.283878	0.246986	0.288879	0.27245
Max	0.979205	0.619943	0.846856	0.65855

TABLE 3. The minimum, 1st quartile, median, mean, 3rd quartile and maximum of the imaginary parts of the first zero of $L(f \otimes \psi_d, s)$ above the central value for $f \in M_2(\Gamma_0(13))$ non self-dual and of non-trivial nebentypus, and for quadratic characters ψ_d of admissible discriminant d .

2.1.3. *Non self-dual, primitive nebentypus.* Let f be a primitive holomorphic cusp form of weight 2 and level 13 and with primitive nebentypus that is not self-dual (LMFDB label: **13.2.e.a**). Let $\mathcal{D}(X)$ be defined as in Definition 4 for $f \neq \bar{f}$. We calculate the distribution of the lowest zero for $L(s, f \otimes \psi_d)$ for $d < X$ for $X = 40000$ and $d \equiv \diamond \pmod{13}$. The basic statistics of the distributions are reported in Table 3 and density plots for the distributions are seen in Figure 3. As expected, the centers of these distributions decrease as d increases.

2.2. **Comparing with Random Matrix Theory predictions.** Now we turn from the raw data associated to twists of these three types of L-functions and to the comparison of these data with the corresponding data from random matrix theory. In this section we do not concern ourselves with excising the model, we pick that up in the next section.

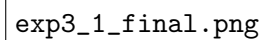
2.2.1. *Matrix groups calculations.* As explained in [\[\[NCR: Section 6.6\]\]](#), just after Corollary 8, the L-functions corresponding to forms f where χ_f is principal correspond to matrices in the group $\mathrm{SO}(\text{even})$, forms f that are self-dual and have non-principal χ_f correspond to matrices in $\mathrm{U}(N)$ [\[\[NCR: even?\]\]](#) and forms f that are not self-dual and have non-principal χ_f correspond to matrices in $\mathrm{USp}(2N)$ [\[\[NCR: even?\]\]](#). We implemented an algorithm for each group in Sage; the algorithm is described in [13]. See Figure 4 for density plots of 100,000 50×50 matrices from each group.

2.2.2. *Trivial nebentypus.* Let f be as in Section 2.1.1. Let $\mathcal{D}_f(X)$ be as in [\[\[NCR: Definition 4\]\]](#) for χ_f principal. We calculate the distribution of the lowest zero for $L(s, f \otimes \psi_d)$ for $d \in \mathcal{D}_f(X)$, provided $L(1/2, f \otimes \psi_d) \neq 0$. We also calculate the distribution of the lowest eigenvalue for $\mathrm{SO}(2N_{\mathrm{std}})$ where N_{std} for discriminants around X is given by

$$N_{\mathrm{std}} = \log \left(\frac{\sqrt{3}X}{2\pi e} \right).$$

In Figure 5 we show the same zeros as in Figure 1 and a plot of the distribution for random matrices in $\mathrm{SO}(8)$ since N_{std} for $X \approx 40,000$ is $3.6 \dots$. The plots have been normalized to as to have the same mean. We observe that the match between the two distributions is pretty good. In a later section we sample differently and get a better fit; see Section 2.3.1.

2.2.3. *Self-dual, non-trivial nebentypus.* Let f be as in Section 2.1.2. Let $\mathcal{D}_f(X)$ be as in [\[\[NCR: Definition 4\]\]](#) for χ_f non-trivial. We calculate the distribution of the lowest zero for $L(s, f \otimes \psi_d)$ for $d \in \mathcal{D}_f(X)$, provided $L(1/2, f \otimes \psi_d) \neq 0$. We also calculate the distribution of the lowest


 The top panel of Figure 3 is a density plot labeled 'exp3_1_final.png'. It shows the distribution of the imaginary parts of the first zero of the L-function $L(f \otimes \psi_d, s)$ for $\varpi = 1$. The plot area is mostly blank, with a very faint horizontal dashed line near the bottom, representing the mean of the distribution.

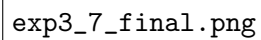

 The bottom panel of Figure 3 is a density plot labeled 'exp3_7_final.png'. It shows the distribution of the imaginary parts of the first zero of the L-function $L(f \otimes \psi_d, s)$ for $\varpi = 2$. Similar to the top panel, the plot area is mostly blank with a very faint horizontal dashed line near the bottom, representing the mean.

FIGURE 3. Density plots of imaginary parts of the first zero of $L(f \otimes \psi_d, s)$ above the central value for $f \in M_2(\Gamma_0(13))$ non self-dual and of non-trivial nebentypus, for quadratic characters ψ_d of admissible discriminant d . The top image is for $\varpi = 1$ and the bottom image is for $\varpi = 2$. The dashed line corresponds to the means of

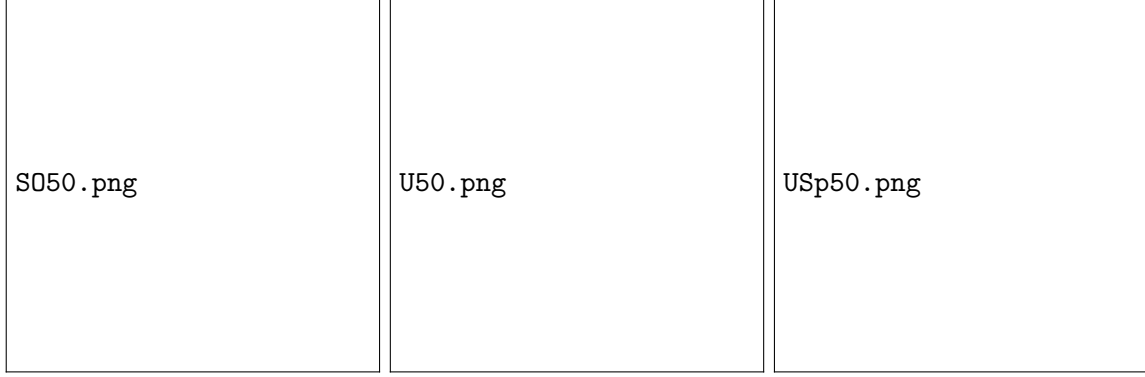


FIGURE 4. Density plots of 100,000 50×50 matrices in (from the left) the special orthogonal group, the unitary and the unitary symplectic group. The shape of the curve matches the predictions in [\[\[NCR: Corollary 8\]\]](#).[\[\[NCR: I need to regenerate nicer plots here\]\]](#)

eigenvalue for $U(N_{\text{std}})$ where N_{std} for discriminants around X is once again given by

$$N_{\text{std}} = \log \left(\frac{\sqrt{3}X}{2\pi e} \right).$$

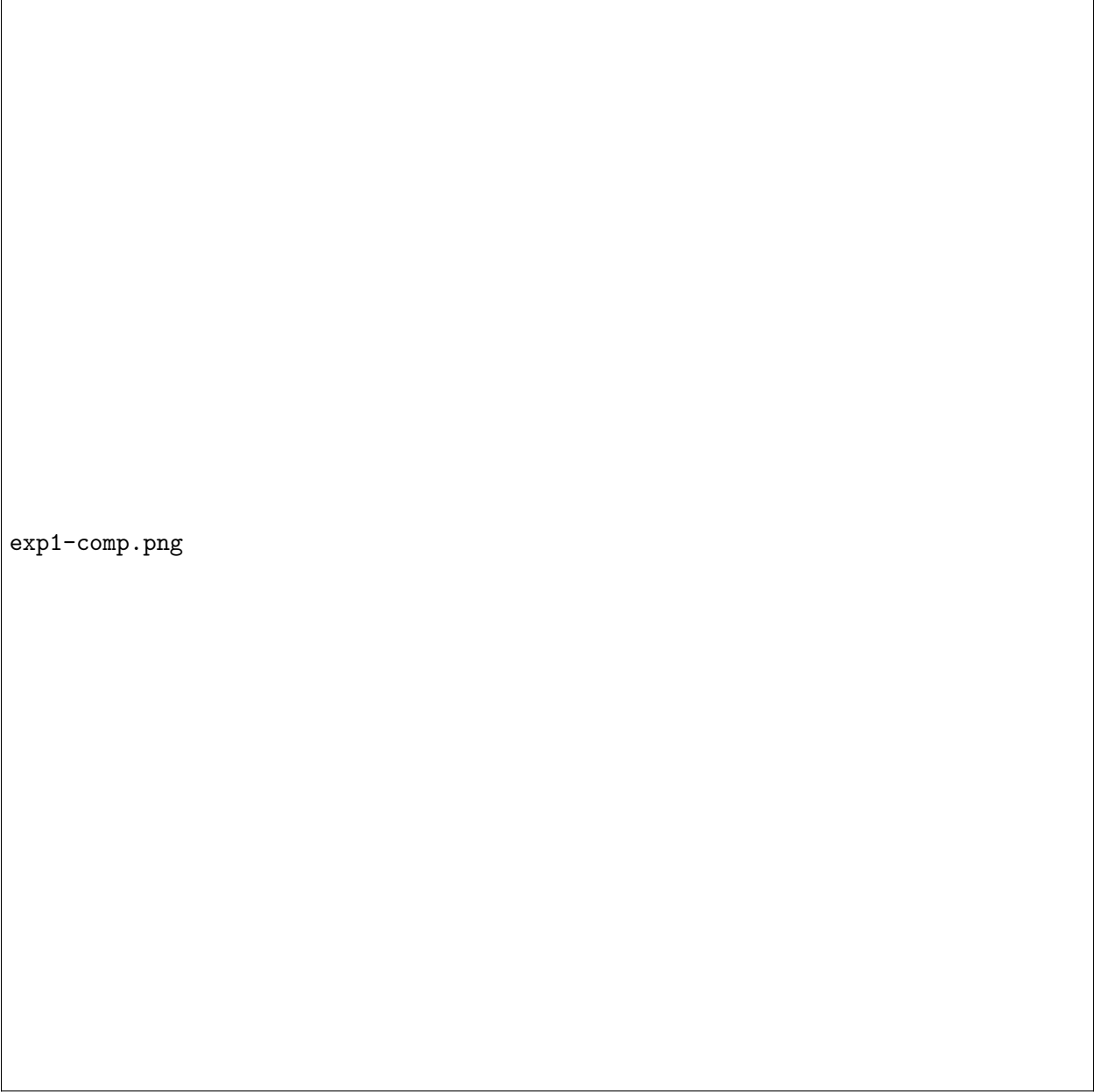
In Figure 6 we show the same zeros as in Figure 1 and a plot of the distribution for random matrices in $U(4)$ since N_{std} for $X \approx 40,000$ is $3.6 \dots$. The plots have been normalized to as to have the same mean. We observe that the match between the two distributions is pretty good.

2.2.4. Non-self-dual, non-trivial nebentypus. Let f be as in Section 2.1.3. Let $\mathcal{D}_f(X)$ be as in [\[\[NCR: Definition 4\]\]](#) for χ_f non-trivial. We calculate the distribution of the lowest zero for $L(s, f \otimes \psi_d)$ for $d \in \mathcal{D}_f(X)$, provided $L(1/2, f \otimes \psi_d) \neq 0$. We also also calculate the distribution of the lowest eigenvalue for $USp(N_{\text{std}})$ where N_{std} for discriminants around X is once again given by

$$N_{\text{std}} = \log \left(\frac{\sqrt{3}X}{2\pi e} \right).$$

In Figure 7 we show the same zeros as in Figure 1 and a plot of the distribution for random matrices in $USp(8)$ since N_{std} for $X \approx 40,000$ is $3.6 \dots$. The plots have been normalized to as to have the same mean. We observe that the match between the two distributions is quite good. [\[\[NCR: Gustavo: según lo que dice Gonzalo esta f s cumple KZ. I me escribi: Este es un ejemplo "famoso", es la primera cuya forma de peso 3/2 que no se puede construir con matrices de brandt / lgebras de cuaterniones definidas. O sea: K-Z y Waldspurger valen en este caso, pero la construccin que hacemos con series theta de formas cuadráticas ternarias \(definidas positivas\) no funciona. Si hay un inters particular por esta forma, habra que trabajar de otra manera para encontrar la forma de peso 3/2 \(por ejemplo, multiplicarla por una de peso 1/2, determinar la de peso 2 resultante, calcularla, y dividir – como hacen Poor y Yuen con las paramodulares – obviamente va a ser ms lento\). No s si te interesa esto pero lo podemos hablar el jueves.\]\]](#)

2.3. Excising the model. While the agreement of the low-lying zeros of L-functions and eigenangles of random matrices illustrated in the last section look pretty good, we would like to carry out an experiment related to the excised model described earlier. In particular, we observe that by Waldspurger’s theorem [23] and, more explicitly by the Kohnen–Zagier formula [11] $L(f \otimes \chi_d, 1/2)$ is discretized. In particular, suppose a modular form of weight 2 corresponds to $h = \sum c(n)q^n$ in



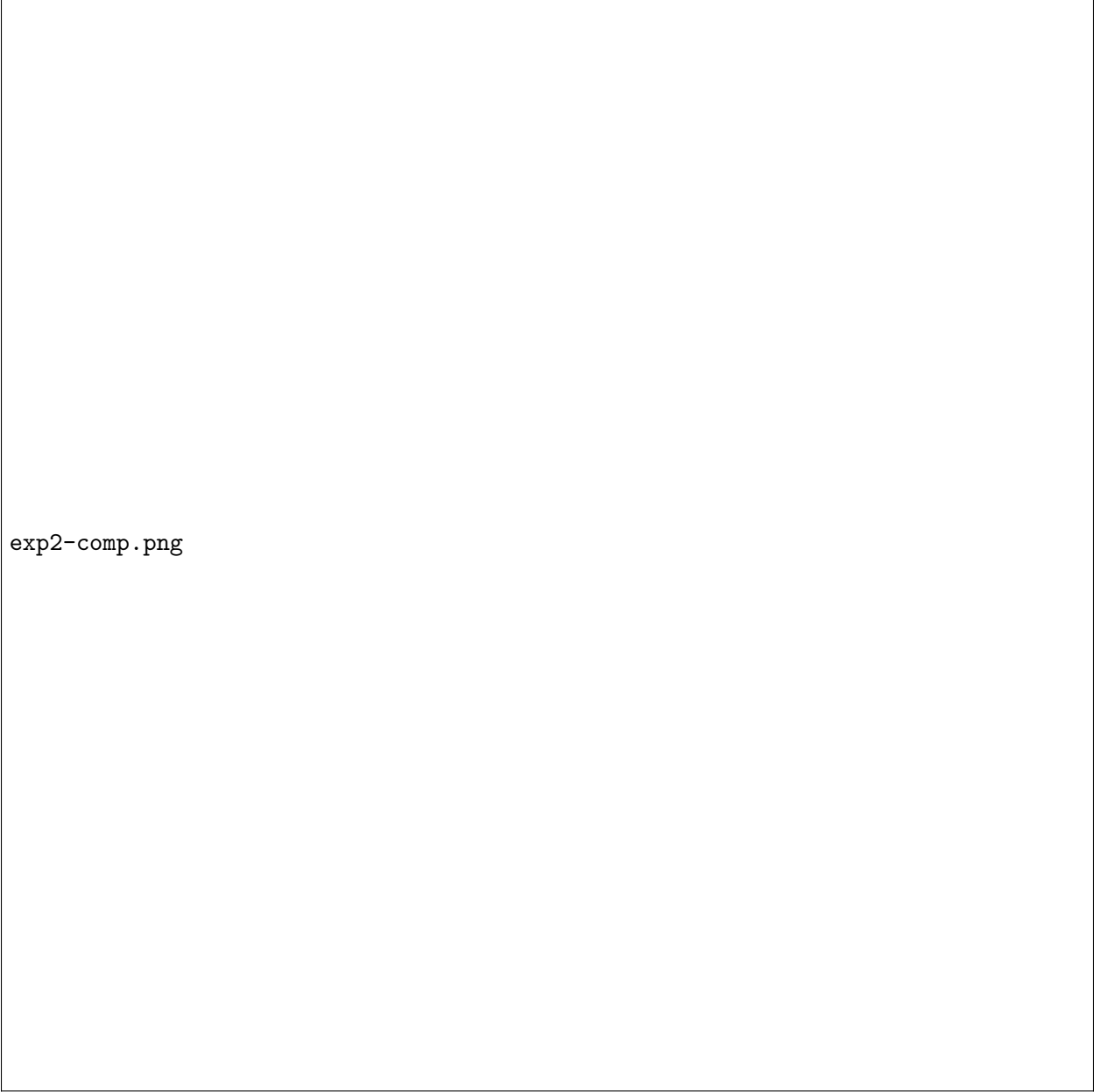
exp1-comp.png

FIGURE 5. A comparison of lowest positive eigenangle in $\mathrm{SO}(8)$ and \mathcal{F}_f where f is as in Section 2.1.1. The two graphs have been normalized to have the same mean.

the Kohnen plus space of weight $3/2$, with $c(n) \in \mathbb{Z}$. Then,

$$L(f \otimes \chi_d, 1/2) = \frac{\kappa_f c(|d|)^2}{|d|^{1/2}},$$

where $\kappa_f > 0$ depends only on f and g and not on χ_d . This means, for example, that if $L(f \otimes \chi_d, 1/2) < \kappa_f |d|^{-1/2}$ then it is equal to zero. And, moreover, it means that for the L-funcitons in the families we are considering (they are rank 0), we know $L(f \otimes \chi_d, 1/2) > \kappa_f |d|^{-1/2}$.



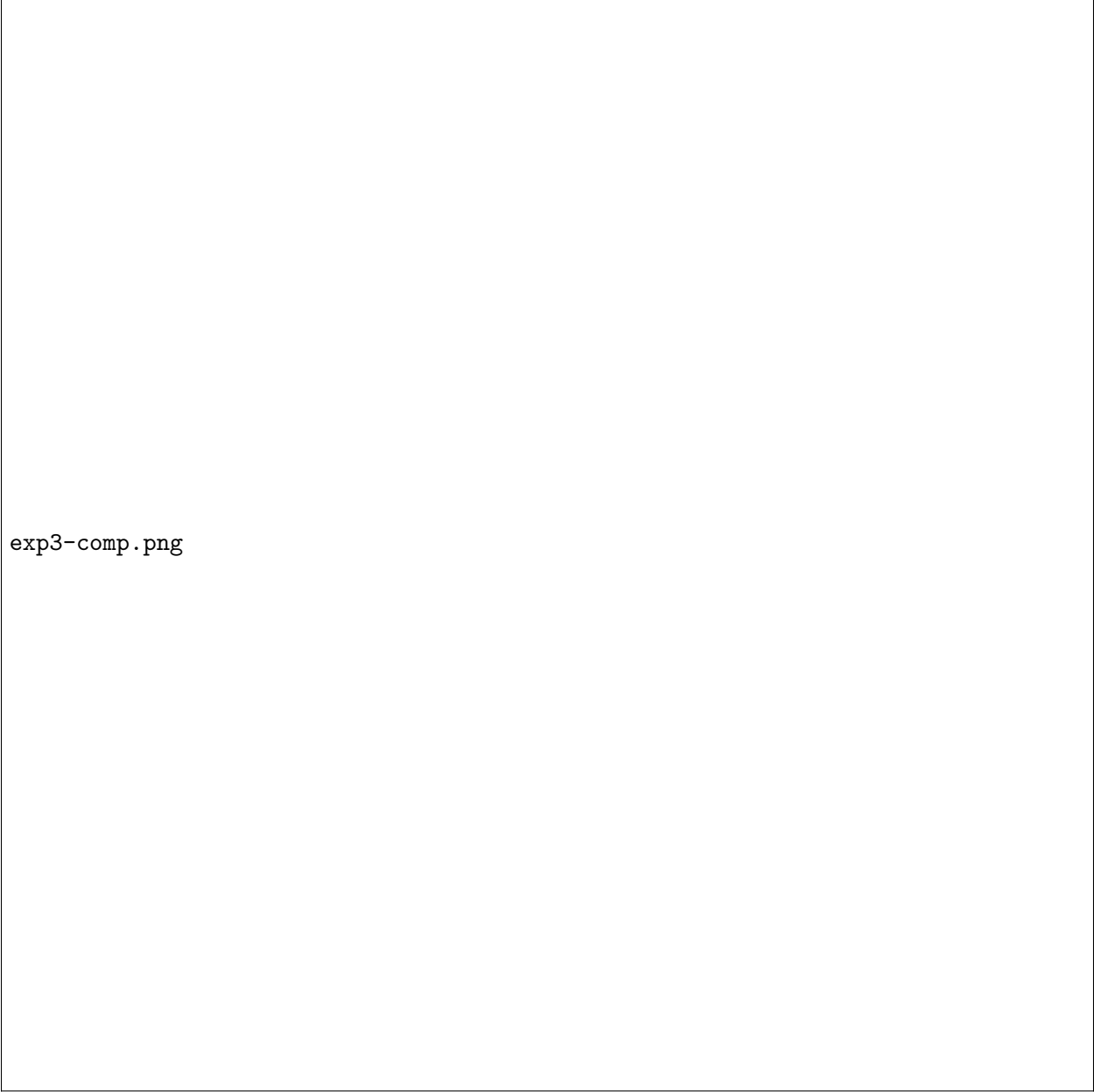
exp2-comp.png

FIGURE 6. A comparison of lowest positive eigenangle in $U(4)$ and \mathcal{F}_f where f is as in Section 2.1.2 and where $\heartsuit = +1$. The two graphs have been normalized to have the same mean.

In the previous sections, we freely sampled from the entire space of random matrices. In this section we sample from a subspace. In [6, 4, 5, 10] it was shown that values of L-functions at the central point can be modeled using characteristic polynomials evaluated at the point 1. So, in analogy with the values $L(f \otimes \chi_d)$ is not allowed to take on, we model rank 0 curves by discarding from our sample space all random matrices A whose characteristic polynomial $\Lambda_A(z, N)$ is away from 0 when evaluated at $z = 1$.

In [\[NCR: Section 3\]](#), it is shown that the cutoff will be of the form

$$|\Lambda_A(1, N)| \geq c_{\text{std}} \times \exp((1 - k)N_{\text{std}}/2)$$



exp3-comp.png

FIGURE 7. A comparison of lowest positive eigenangle in $U(4)$ and \mathcal{F}_f where f is as in Section 2.1.3 and where $\diamond = 7$. The two graphs have been normalized to have the same mean.

and in this section we estimate the constant c_{std} for each of the three cases and leave, for two of the three cases, the verification of whether or not our approximation matches the formula given in [\[\[NCR: \(3.23\)\]\]](#) for future work.

2.3.1. *Trivial nebentypus.* In this section we consider forms of weights 4, 6, 8 and 10 [\[\[NCR: these weights? others?\]\]](#) and study how well the low-lying zeros of their associated L-functions are modelled using the excised model. In particular, we approximate the choice of c_{std} and the calculate explicitly using [\[\[NCR: \(3.23\)\]\]](#). See Table 4 for the forms that we use.

Weight	Label	f	g	κ_f	# coeffs	$\mathcal{L}_M(X, f)$
4						
6						
8						
10						

TABLE 4. A table of the forms f for which we calculate c_{std} . We report the form's LMFDB label, the first few coefficients of f , the first few coefficients of the Shimura lift g of f , the constant κ_f in the Kohnen-Zagier formula and the number of coefficients we can calculate for g . We also report the local factor of the L-function at M , the level of f .

To find the value of c_{std} numerically, we proceed as follows. Let f be the form we are considering and suppose it is of level N . Calculate as many central values of $L(f \otimes \psi_d, 1/2)$ as possible (see Table 4). Let N_{std} be the size of the group of random matrices used to model the zeros of f . Let c be a candidate value for c_{std} . Then we calculate a sample of 10^7 matrices A [\[NCR: I don't know that this will be enough\]](#) in $SO(2N_{\text{std}})$ such that $\Lambda_A(1, N_{\text{std}}) \geq c \exp((1-k)N_{\text{std}}/2)$ [\[NCR: Gustavo: Todo esto se puede hacer fácilmente en R, las matrices, los polinomios característicos, etc.\]](#). Then for this c we compare the distribution of zeros and eigenangles. In particular, we measure the agreement between the distribution of the central values and the distribution of the characteristic polynomials evaluated at 1 by averaging the absolute value of the difference between the cumulative distribution of the zeros and the cumulative distribution of the eigenvalues at a set of evenly spaced points. [\[NCR: Gustavo: No sé si hace falta normalizar para que tengan el mismo medio o mediano\]](#) See Figure ?? for what such a plot might look like. See Table 5 for a summary of our results.

As further confirmation, we compute c_{std} using the following formula:

$$c_{\text{std}} \times \exp((1-k)N_{\text{std}}/2) := a_f^{-2}(-1/2) \delta_f \kappa_f \times \exp((1-k)N_{\text{std}}/2)$$

where κ_f is the constant in the Kohnen-Zagier formula,

$$a_f(m) = \left[\prod_p \left(1 - \frac{1}{p}\right)^{m(m-1)/2} \right] \times \left[\prod_{p|M} \left(1 + \frac{1}{p}\right)^{-1} \left(\frac{1}{p} + \frac{1}{2} \left[\mathcal{L}_p(p^{-1/2}, f)^m + \mathcal{L}_p(-p^{-1/2}, f)^m \right] \right) \right] \times \mathcal{L}_M \left(\frac{\epsilon_f}{M^{1/2}}, f \right)^m$$

and

$$\sqrt{\delta_f} = \frac{|\{L(f \otimes \psi_d, s) \in \mathcal{F}_f : d \text{ prime}, L(f \otimes \psi_d, 1/2) = 0\}|}{\sum_{d \text{ prime}}^* 2a_f(-1/2) \sqrt{\kappa_f} d^{(1-k)/4} h(\log d)}.$$

Label	$a_f(1/2)$	δ_f	N_{std}	# matrices	c_{std} approx	c_{std} formula

TABLE 5. A table of results, intermediate and final, related to find c_{std} for the f in Table 4.

Here [\[\[NCR: eigenvalues are normalized by dividing by \$p^{\(k-1\)/2}\$ \]\]](#)[\[\[NCR: in the paper there is a + superscript on \$\mathcal{D}\$ and \$\mathcal{F}\$ sometimes\]\]](#)[\[\[NCR: I think \$\chi_f\(p\) = 1/p\$ \]\]](#)

$$\mathcal{L}_p(X, f) = (1 - \lambda_f(p)X + \chi_f(p)X^2)^{-1}$$

$$\mathcal{F}_f(X) = \{L(f \otimes \psi_d, s) : d \in \mathcal{D}_f(X)\}$$

$$\mathcal{D}_f(X) = \{d \text{ fundamental} : 0 < d \leq X \text{ and } \psi_d(M)\epsilon_f = +1\}$$

$$\mathcal{F}_f = \lim_{X \rightarrow \infty} \mathcal{F}_f(X)$$

$$\sum^* = \text{sum } d \text{ fundamental, prime such that } f \otimes \psi_d \text{ has an even functional equation,}$$

$$h(N) = 2^{-N} \Gamma(N)^{-1} \prod_{j=1}^N \frac{\Gamma(N+j-1)\Gamma(j)}{\Gamma(j-1/2)\Gamma(j+N-3/2)}.$$

To do:

- find the constant in KZ
- compute lots of coeffs of the Shimura lift
- compute lots of central values
- compute lots of excised matrices and for various values of c
- scale them so the means or medians are the same
- make a plot like in [7]

Approximate c_{std} as described above.

2.3.2. Self-dual, non trivial nebentypus. No analogue of KZ.

To do:

- compute $L(f \otimes \chi_d, 1/2)$ for the same f as above.
- compute lots of excised matrices andfor various values of c
- scale them so the means or medians are the same
- make a plot like in [7]

Approximate c_{std} as described above.

2.3.3. Non self-dual, primitive nebentypus. No analogue of KZ.

To do:

- compute $L(f \otimes \chi_d, 1/2)$ for the same f as above.
- compute lots of excised matrices andfor various values of c
- scale them so the means or medians are the same
- make a plot like in [7]

Approximate c_{std} as described above.

REFERENCES

- [1] Owen Barrett and Steven J. Miller. An excised orthogonal model for families of cusp forms. Preprint.
- [2] Eugene B Bogomolny and Jon Peter Keating. Random matrix theory and the riemann zeros. i. three-and four-point correlations. *Nonlinearity*, 8(6):1115, 1995.

- [3] Eugene B Bogomolny and Jonathan P Keating. Random matrix theory and the riemann zeros ii: n-point correlations. *Nonlinearity*, 9(4):911, 1996.
- [4] J. B. Conrey, J. P. Keating, M. O. Rubinstein, and N. C. Snaith. On the frequency of vanishing of quadratic twists of modular L -functions. In *Number theory for the millennium, I (Urbana, IL, 2000)*, pages 301–315. A K Peters, Natick, MA, 2002.
- [5] J Brian Conrey, Jon P Keating, Michael O Rubinstein, and Nina C Snaith. Random matrix theory and the fourier coefficients of half-integral-weight forms. *Experimental Mathematics*, 15(1):67–82, 2006.
- [6] JB Conrey and DW Farmer. Mean values of l-functions and symmetry. *International Mathematics Research Notices*, 2000(17):883–908, 2000.
- [7] E. Dueñez, D. K. Huynh, J. P. Keating, S. J. Miller, and N. C. Snaith. A random matrix model for elliptic curve L -functions of finite conductor. *J. Phys. A*, 45(11):115207, 32, 2012.
- [8] Henryk Iwaniec, Wenzhi Luo, and Peter Sarnak. Low lying zeros of families of l -functions. *Publications Mathématiques de l’IHÉS*, 91:55–131, 2000.
- [9] Nicholas Katz and Peter Sarnak. Zeroes of zeta functions and symmetry. *Bulletin of the American Mathematical Society*, 36(1):1–26, 1999.
- [10] Jon P Keating and Nina C Snaith. Random matrix theory and L -functions at $s = 1/2$. *Communications in Mathematical Physics*, 214(1):91–100, 2000.
- [11] Winfried Kohnen and Don Zagier. Values of L -series of modular forms at the center of the critical strip. *Inventiones mathematicae*, 64(2):175–198, 1981.
- [12] The LMFDB Collaboration. The L -functions and modular forms database. <http://www.lmfdb.org>, 2020. [Online; accessed 5 July 2020].
- [13] Francesco Mezzadri. How to generate random matrices from the classical compact groups. *Notices Amer. Math. Soc.*, 54(5):592–604, 2007.
- [14] Steven J. Miller. Investigations of zeros near the central point of elliptic curve L -functions. *Experiment. Math.*, 15(3):257–279, 2006. With an appendix by Eduardo Dueñez.
- [15] Hugh L Montgomery. The pair correlation of zeros of the zeta function. In *Proc. Symp. Pure Math*, volume 24, pages 181–193, 1973.
- [16] AM Odlyzko. The 10^{22} -nd zero of the riemann zeta function. *Dynamical, Spectral, and Arithmetic Zeta Functions: AMS Special Session on Dynamical, Spectral, and Arithmetic Zeta Functions, January 15-16, 1999, San Antonio, Texas*, 290:139, 2001.
- [17] Ali Erhan Özlük and Chip Snyder. On the distribution of the nontrivial zeros of quadratic l -functions close to the real axis. *Acta Arithmetica*, 91(3):209–228, 1999.
- [18] R Core Team. *R: A Language and Environment for Statistical Computing*. R Foundation for Statistical Computing, Vienna, Austria, 2018.
- [19] Zeév Rudnick, Peter Sarnak, et al. Zeros of principal l -functions and random matrix theory. *Duke Mathematical Journal*, 81(2):269–322, 1996.
- [20] Nathan C. Ryan. Repulsion of low-lying zeros of l -functions. <https://github.com/nathancryan/vanishings>, 2019.
- [21] W.A. Stein et al. *Sage Mathematics Software (Version 7.2)*. The Sage Development Team, 2016. <http://www.sagemath.org>.
- [22] The PARI Group, Univ. Bordeaux. *PARI/GP version 2.11.2*, 2018. available from <http://pari.math.u-bordeaux.fr/>.
- [23] J-L Waldspurger. Sur les valeurs de certaines fonctions L automorphes en leur centre de symétrie. *Compositio Mathematica*, 54(2):173–242, 1985.

UNIVERSIDAD SAN FRANCISCO DE QUITO, CUMBAYÁ, ECUADOR
E-mail address: xxx

UNIVERSIDAD SAN FRANCISCO DE QUITO, CUMBAYÁ, ECUADOR
E-mail address: xxx

UNIVERSIDAD DE LA REPÚBLICA, MONTEVIDEO, URUGUAY
E-mail address: grama@fing.edu.uy

BUCKNELL UNIVERSITY, LEWISBURG, PENNSYLVANIA, USA
E-mail address: nathan.ryan@bucknell.edu